

PAPER

CMOS MEMS capacitive absolute pressure sensor

To cite this article: M Narducci *et al* 2013 *J. Micromech. Microeng.* **23** 055007

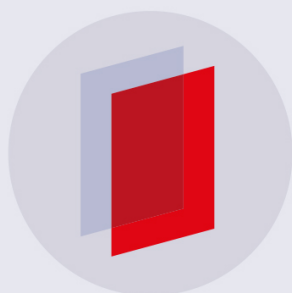
View the [article online](#) for updates and enhancements.

Related content

- [Monolithic integration of capacitive sensors using a double-side CMOS MEMS post process](#)
Chih-Ming Sun, Chuanwei Wang, Ming-Han Tsai *et al.*
- [A new process for CMOS MEMS capacitive sensors with high sensitivity and thermal stability](#)
S S Tan, C Y Liu, L K Yeh *et al.*
- [A 100 \$\mu\$ m diameter capacitive pressure sensor with 50 MPa dynamic range](#)
Xin Luo and Yogesh B Gianchandani

Recent citations

- [Design, fabrication and optimization of a CMOS compatible capacitive pressure sensor](#)
Huiyang Yu *et al*
- [Touch-mode capacitive pressure sensor with graphene-polymer heterostructure membrane](#)
Christian Berger *et al*
- [The capacitive proximity sensor based on transients in RC-circuits](#)
A G Yakunin



IOP | ebooks™

Bringing you innovative digital publishing with leading voices to create your essential collection of books in STEM research.

Start exploring the collection - download the first chapter of every title for free.

CMOS MEMS capacitive absolute pressure sensor

M Narducci¹, L Yu-Chia², W Fang³ and J Tsai^{1,4}

¹ Institute of Microelectronics, A*STAR (Agency for Science, Technology and Research), Singapore

² Institute of NanoEngineering and MicroSystems, National Tsing Hua University, Hsinchu, Taiwan

³ Department of Power Mechanical Engineering, National Tsing Hua University, Hsinchu, Taiwan

⁴ Department of Electrical and Computer Engineering, National University of Singapore, Singapore

E-mail: narduccims@ime.a-star.edu.sg

Received 20 November 2012, in final form 25 February 2013

Published 25 March 2013

Online at stacks.iop.org/JMM/23/055007

Abstract

This paper presents the design, fabrication and characterization of a capacitive pressure sensor using a commercial 0.18 μm CMOS (complementary metal–oxide–semiconductor) process and postprocess. The pressure sensor is capacitive and the structure is formed by an Al top electrode enclosed in a suspended SiO_2 membrane, which acts as a movable electrode against a bottom or stationary Al electrode fixed on the SiO_2 substrate. Both the movable and fixed electrodes form a variable parallel plate capacitor, whose capacitance varies with the applied pressure on the surface. In order to release the membranes the CMOS layers need to be applied postprocess and this mainly consists of four steps: (1) deposition and patterning of PECVD (plasma-enhanced chemical vapor deposition) oxide to protect CMOS pads and to open the pressure sensor top surface, (2) etching of the sacrificial layer to release the suspended membrane, (3) deposition of PECVD oxide to seal the etching holes and creating vacuum inside the gap, and finally (4) etching of the passivation oxide to open the pads and allow electrical connections. This sensor design and fabrication is suitable to obey the design rules of a CMOS foundry and since it only uses low-temperature processes, it allows monolithic integration with other types of CMOS compatible sensors and IC (integrated circuit) interface on a single chip. Experimental results showed that the pressure sensor has a highly linear sensitivity of 0.14 fF kPa^{-1} in the pressure range of 0–300 kPa.

(Some figures may appear in colour only in the online journal)

1. Introduction

MEMS (microelectromechanical systems) pressure sensors provide the advantages of high performance, small size, light weight and low cost. Several types of MEMS sensors have been studied to detect pressure, for instance, capacitive, piezoresistive, resonant and fiber optic, on which capacitive pressure sensors are one of the most widely studied devices for different types of applications such as biomedical, automotive and aerospace. Ko *et al* [1, 2] fabricated a tactile sensor to recognize fingerprints. Buyong *et al* [3] developed a sensor to evaluate pressure in the eye for glaucoma analysis. Dai *et al* [4] and Sun *et al* [5] presented a sensor to measure the tire pressure in an automobile. MEMS capacitive sensors provide high pressure sensitivity, low noise, low power consumption and

low temperature sensitivity. The critical constrains for MEMS capacitive sensors are nonlinearity for large displacement and the low signal level; therefore a parallel plate structure with small displacement (in the pressure range of interest) and incorporating on-chip amplification and noise suppression would be an optimal solution. In order to guarantee on-chip integration of the IC (integrated circuit) and the MEMS pressure sensor, the CMOS (complementary metal–oxide–semiconductor) MEMS technique needs to be employed for fabrication [6–9].

This paper presents the fabrication and characterization of a CMOS MEMS capacitive pressure sensor that allows monolithic integration with other type of CMOS compatible sensors and IC interface on a single chip.

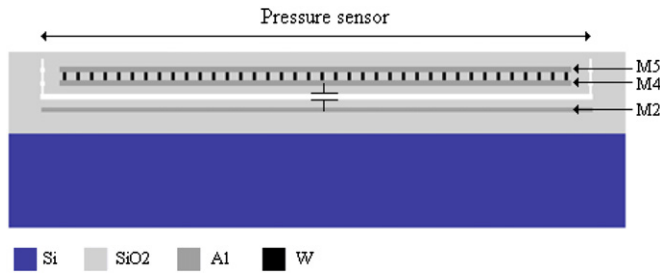


Figure 1. Cross-sectional view of the CMOS MEMS pressure sensor.

2. Pressure sensor structure

Capacitive pressure sensors measure the capacitance between two electrodes with variable separation due to a moving membrane or sensing element. The basic structure of a capacitor consists of a set of parallel plates or electrodes of area A , separated by a distance d . The value of the capacitance is given by the following equation [10, 11]:

$$C = \epsilon A/d \tag{1}$$

where ϵ is the dielectric constant of the medium between the plates.

The structure illustrated in figure 1 shows the cross-sectional view of a pressure sensor using dielectric and metal layers of the CMOS process. As can be seen from the figure, the movable electrode, or suspended membrane, is formed by two metal layers (M-4, M-5), three intermetal dielectric (IMD3, IMD4 and IMD5), and multiple VIAS connecting M-4 and M-5 in parallel in order to increase the stiffness of the membrane. The stationary electrode is fixed on the substrate formed by the metal layer M-2 and covered by the intermetal dielectric IMD2. In order to create the gap between the electrodes, the metal M-3 is used as a sacrificial layer and stacks of VIAS and metals are used to access it.

Using this approach the capacitance is formed between metals M-2 and M-4, with the dielectric formed by an air gap and intermetal dielectrics IMD2 and IMD3. If a pressure load is applied, the suspended membrane is deformed and the air gap is reduced causing a variation on the value of the capacitor.

3. Fabrication process

The CMOS is fabricated using a 0.18 μm technology of GLOBAL-FOUNDRIES. The use of the CMOS-MEMS technique, to design the pressure sensor, requires obeying the design rules of the CMOS foundry. Also, in order to guaranty the CMOS compatibly, only low-temperature postprocess can be used to release the suspended membrane (figure 2 illustrates the fabrication process flow of the CMOS MEMS pressure sensor). After the completion of the CMOS, in order to protect the pads a SiO_2 layer is deposited and patterned (mask1) to cover everything except for the pressure sensor area (figure 2(a)). The next step is to etch the sacrificial stacked layer and release the suspended membrane (figure 2(b)). In order to etch the stacked metal (>99% aluminum) and via (tungsten) layers, a $\text{H}_2\text{SO}_4 + \text{H}_2\text{O}_2$ solution is used to do

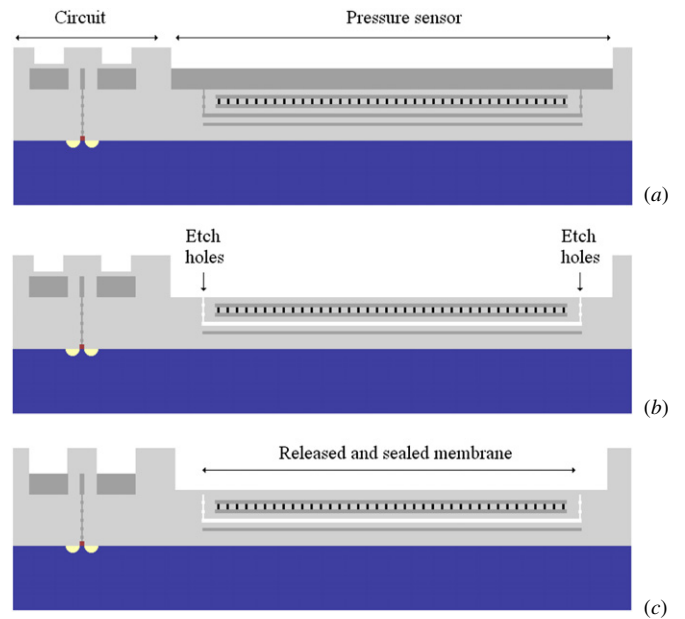


Figure 2. CMOS MEMS pressure sensor fabrication process flow: (a) after the completion of the CMOS and pad protection. (b) After the etching of the sacrificial stacked layers. (c) After the sealing of the etching holes and pad opening.

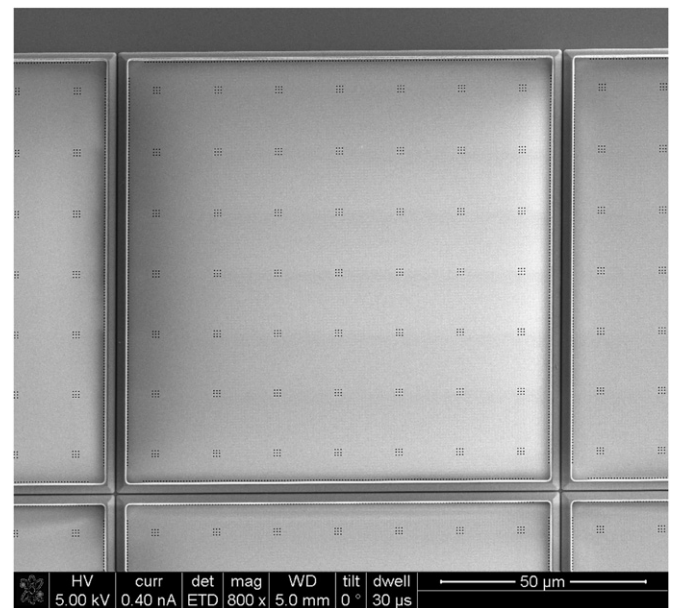


Figure 3. SEM (scanning electron microscope) photograph of the top view of the released membrane.

the release. During the etching of the sacrificial layer, the dielectric acts as a stopping layer protecting top and bottom electrodes, electrical connections and IC, if required. After the release of the membrane, low-stress oxide is deposited in order to seal the etching holes (figure 2(c)). The etching holes are sealed under a vacuum chamber, so the cavity under the membrane is nearly in vacuum (~ 6 mTorr). Finally, using photolithography and RIE (reactive ion etching) the oxide is patterned (mask2) in order to open the pads to allow electrical connections (figure 2(c)). Figure 3 shows the top view of the released membrane, each with an area of 110 by 110 μm ; in this photograph the distribution of release holes

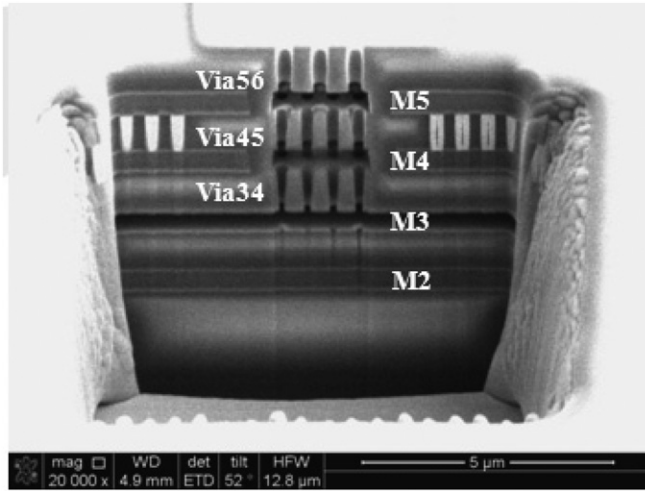


Figure 4. SEM photograph of the cross-sectional view of the released membrane.

Table 1. Material properties used in this work.

Property	Al	SiO ₂
Mass density (kg μ ⁻³)	2.3 × 10 ⁻¹⁵	2.15 × 10 ⁻¹⁵
Young's modulus (GPa)	77	70
Poisson's ratio	0.3	0.17

can be observed. Figure 4 shows the cross-sectional view of the release holes and the gap with no stiction between the movable and stationary electrode. Each structure after sealing contains, from bottom to top, 0.54 μm of Al (M-2), 0.9 μm of SiO₂ (IMD2), 0.54 μm of air gap (equivalent to M-3), 0.9 μm of SiO₂ (IMD3), 0.54 μm of Al (M-4), 0.9 μm of SiO₂ (IMD4), 0.54 μm of Al (M-5), 0.9 μm of SiO₂ (IMD5) and 0,6 μm of SiO₂ (sealing oxide). A very important aspect to take into account would be the reproducibility of the thicknesses of the layers that define the gap between the bottom and top electrodes and the layers that define the movable membrane. A small variation in each layer can lead to different results and therefore lack of precision. Further study should be done in order to guarantee the reproducibility of the sensor [12, 13, 14].

4. Simulation results

The finite element method software COVENTOR was used to simulate the behavior of the sensor under different loads conditions (pressure and temperature) applied to the membrane. The 3D model is composed by bottom electrode with oxide layer, the oxide membrane with the top electrode and the sealing oxide layer. In order to simplify the model and reduce computational time, VIAS and etching holes were not included. The boundary conditions are that each edge of the membrane is fixed and that the oxide is subjected to a residual stress of $S_x = S_z = -100$ MPa due to the CMOS fabrication process. The applied loading force is a uniform pressure applied on the membrane. The material properties of the SiO₂ and Al are contained in table 1.

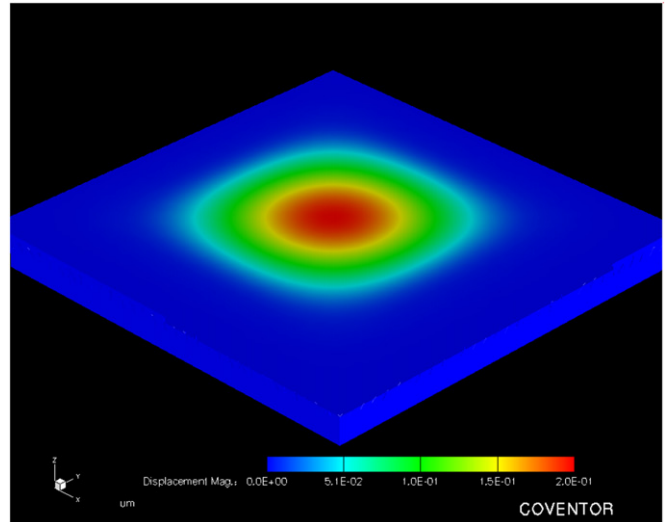


Figure 5. Simulated displacement distribution for an applied pressure of 300 kPa.

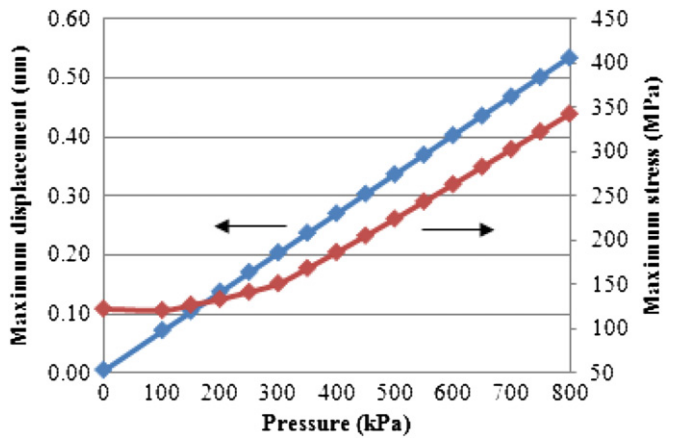


Figure 6. Relationship between displacement (left) and maximum stress (right).

Analytical results include displacement, stress and capacitance extraction. Figure 5 shows the displacement distribution of the membrane for an applied pressure of 300 kPa. The maximum displacement is found to be 0.2 μm in the center of the membrane figure 6 shows the relationship between the displacement and maximum stress for an applied pressure range of 0–800 kPa. For this pressure range, the maximum stress is found to be below the fracture strength of the SiO₂ (0.5–0.9 GPa) and the Al (0.4–0.6 GPa), ensuring that this way the membrane is going to operate in an elastic region [15].

The value of the capacitance (C_s) and how this is going to vary with the pressure (S) was also simulated, obtaining a C_s value of 95.9 fF. Since the value of the capacitance and its variation is too small the readout circuits cannot exactly convert the sensing signal into voltage output; therefore an array of capacitive sensors is required. In this example, for a 3 by 3 array of capacitive sensors in parallel, a C_s of 863.1 fF is obtained. Figure 7(a) shows the nonlinear relationship

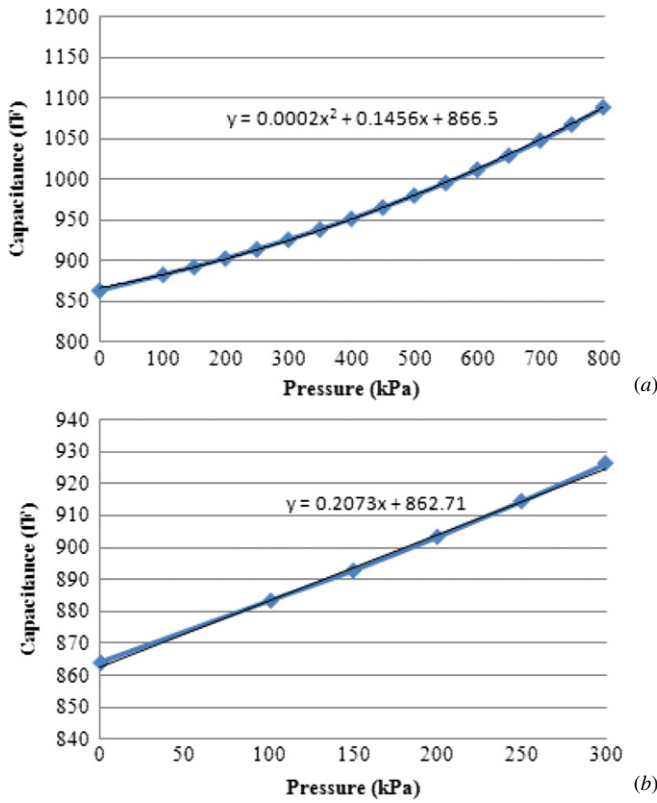


Figure 7. Capacitance versus pressure: (a) pressure range 0–800 kPa, (b) pressure range 0–300 kPa.

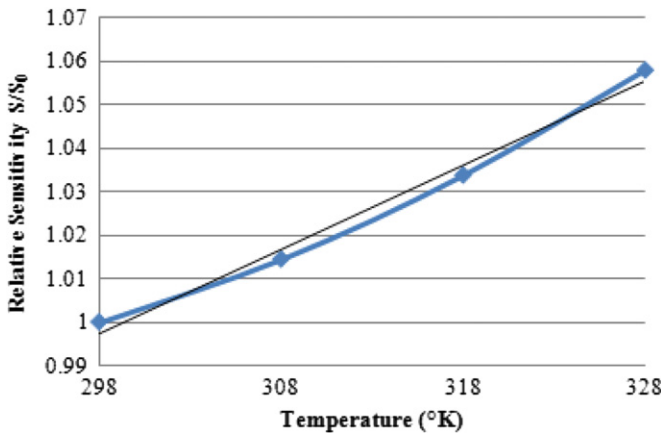


Figure 8. Pressure sensitivity versus temperature.

between C_s and the pressure for a range of 0–700 kPa. In order to obtain a linear response, the pressure range is limited to 0–300 kPa (figure 7(b)), obtaining this way a sensitivity value of ~ 0.2 fF kPa^{-1} . Figure 8 shows the relationship between relative sensitivity and temperature. As can be seen from figure 8, sensitivity would change less than 6%, in the temperature range of interest (298–328 $^{\circ}K$).

5. Experimental results

Figure 9 shows the setup used to test the functionality of the fabricated devices. The packaged sensor is mounted inside a

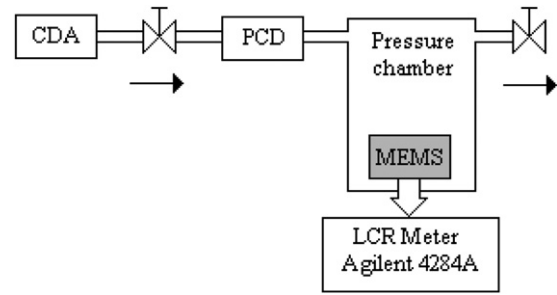


Figure 9. Test setup.

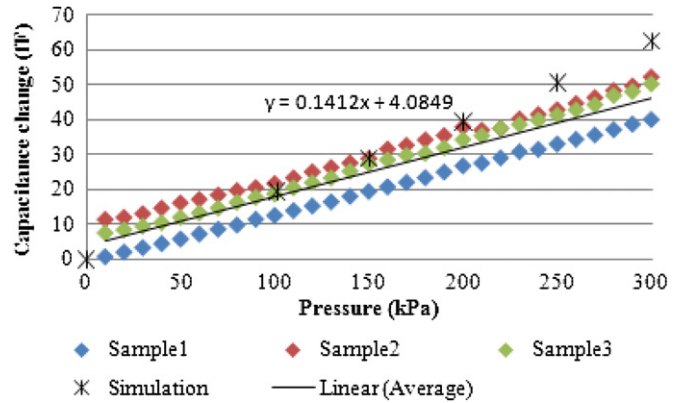


Figure 10. Measured results of the pressure sensor: dependence of capacitance change on applied pressure.

pressure chamber, and the metal pads corresponding to the bottom and top electrodes are connected to an Agilent 4284A precision LCR meter in order to measure the C_s value. An ac bias voltage of 100 mV at frequency of 1 MHz is applied to the structure. Compressed dry air (CDA) is applied to the pressure sensor chamber and the gas pressure is tuned by a PCD ALICAT digital pressure controller. The pressure was swept from 0 to 300 kPa.

The C_s value was measured to be around 2.2 pF; the difference between the simulated value (0.86 pF) and the measured can be attributed to the parasitic effect due to in-chip interconnections and wire bonding. Figure 10 shows the characterization results (variation of C_s versus applied pressure) of three samples and simulation results, showing a measured sensitivity of ~ 0.14 fF kPa^{-1} . Averaged experimental results showed good agreement with simulated ones (0.2 fF kPa^{-1}), taking into account that a simplified 3D model was used in order to reduce computational time.

6. Conclusions and future work

This research has explored the capabilities of a fabrication process for a CMOS-MEMS parallel plate capacitive pressure sensor using a commercial 0.18 μm CMOS process and design rules of the company GLOBAL-FOUNDRIES. The device used consisted of a 3×3 array of capacitive sensors. Experimental results showed a linear response in the range of

0–300 kPa and a sensitivity of 0.14 fF kPa^{-1} . Fabrication results demonstrated that the structure was successfully released with no stiction. Conclusively, this CMOS-MEMS pressure sensor can be fabricated and monolithically integrated on a single chip using the described fabrication process. In the future, the in-chip readout circuit would be designed and characterized. Also, future work will encompass redesign the structure in order to improve the mechanical design to increase the displacement of the membrane due to pressure, leading to better sensitivity taking special considerations in the introduction of nonlinearities. Also, redesigning the structure to increase the value of C_s would enlarge the level of the output signal and this also is going to increase the sensitivity and to reduce the complexity of the circuitry. Further work would also include the optimization of the process variability in order to guarantee the reproducibility of the sensor.

Acknowledgment

This work was supported by the Science and Engineering Research Council of A*STAR (Agency for Science, Technology and Research), Singapore, under the grant no 102 148 0002.

References

- [1] Ko C-T, Wu I-P, Wang W-C, Huang C-H, Tseng S-H, Chen Y-L and Lu M S-C 2006 *Proc. MEMS* pp 642–5
- [2] Hsiung Y-S and Lu M S -C 2011 *Proc. Transducers* pp 24–27
- [3] Buyong M R, Aziz N A and Majlis B Y 2011 *Sains Malaysiana* **40** 259–66
- [4] Dai C-L and Liu M-C 2007 *Japan. J. Appl. Phys.* **46** 843–8
- [5] Sun C-M, Tsai M-H, Wang C, Liu Y-C and Fang W 2009 *Proc. Transducers* pp 1730–3
- [6] Chen P-J, Saati S, Varma R, Humayun M and Tai Y-C 2010 *J. Microelectromech. Syst.* **19** 721–34
- [7] Le H-P, Shah K, Singh J and Zayegh A 2005 *Analog Integr. Circuits Signal Process.* **48** 21–31
- [8] Sun C-M, Wang C, Tsai M-H, Hsieh H-S and Fang W 2009 *J. Micromech. Microeng.* **19** 015023
- [9] Wang C-C, Gogoi B-P, Monk D-J and Mastrangelo C-H 2000 *J. Microelectromech. Syst.* **9** 538–543
- [10] Dai C-L, Lu P-W, Chang C and Liu C-H 2009 *Sensors* **9** 10158–70
- [11] Puers R 1993 *Sensors Actuators A* **37–38** 93–105
- [12] Vaganov V 2010 *Sensors Actuators* **1** 17–30
- [13] Tsai M-H, Sun C-M, Liu Y-C, Wang C and fang W 2009 *J. Micromech. Microeng.* **19** 005017
- [14] Buyong M R, Aziz N A and Majlis B Y 2009 *Adv. Mater. Res.* **74** 231–4
- [15] Chu J and Zhang D 2009 *J. Micromech. Microeng.* **19** 095020